

# ChemComm

Accepted Manuscript



This is an *Accepted Manuscript*, which has been through the Royal Society of Chemistry peer review process and has been accepted for publication.

*Accepted Manuscripts* are published online shortly after acceptance, before technical editing, formatting and proof reading. Using this free service, authors can make their results available to the community, in citable form, before we publish the edited article. We will replace this *Accepted Manuscript* with the edited and formatted *Advance Article* as soon as it is available.

You can find more information about *Accepted Manuscripts* in the [Information for Authors](#).

Please note that technical editing may introduce minor changes to the text and/or graphics, which may alter content. The journal's standard [Terms & Conditions](#) and the [Ethical guidelines](#) still apply. In no event shall the Royal Society of Chemistry be held responsible for any errors or omissions in this *Accepted Manuscript* or any consequences arising from the use of any information it contains.

## COMMUNICATION

## Polymer membrane wearing a mineral coating for enhanced curling resistance and surface wettability

Cite this: DOI: 10.1039/x0xx00000x

Hao-Cheng Yang, Yi-Fu Chen, Chen Ye, Yi-Ning Jin, Hanying Li and Zhi-Kang Xu\*

Received 00th January 2012,

Accepted 00th January 2012

DOI: 10.1039/x0xx00000x

www.rsc.org/

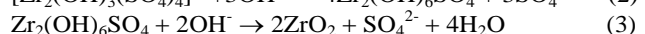
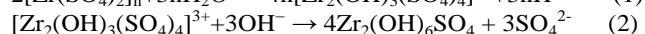
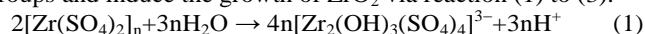
**Zirconia-wrapped membranes have been fabricated via a mineralization process on polydopamine/polyethyleneimine-deposited surfaces. The rigid and hydrophilic mineral coating endows the membranes with enhanced curling resistance and surface wettability simultaneously, enabling the membranes to separate oil-in-water emulsions.**

Advanced polymer membranes have attracted much attention for their increasing demands in water treatment, energy development and health care.<sup>1-3</sup> These membranes are generally used as semi-permeable filters for water purification<sup>4</sup> and ion-conducting separators in lithium ion batteries.<sup>2,5</sup> However, most of them are usually suffering from some undesired drawbacks due to their poor surface wettability to liquids. The poor wettability always leads to a decrease of permeation flux by surface fouling for filtration membranes, and then results in an increased energy consumption and maintenance cost.<sup>6</sup> Likewise, the poor wettability will decrease the uptake and retention of liquid electrolyte in the porous separator, and then impair the battery performance.<sup>5</sup> To address these issues, various approaches have been developed over the past years to hydrophilize the membrane surfaces.<sup>7-12</sup> Although these methods are greatly promising for wettability improvement, an unfavorable issue is shrinkage and curling of the membranes, especially for those membranes with high porosity (Fig. S1, ESI†).<sup>13,14</sup> These phenomena arise from the capillary pressure in the membrane pores as well as the soft nature of the polymeric skeleton. They are particularly detrimental to membrane preparation, surface modification and practical application, which make the improvement in both structure stability and surface wettability a major challenge for advanced membranes. Just like a proverb says, “you cannot have your cake and eat it too”.

The sophisticated structures in nature are a source of inspiration for us to address the above-mentioned issues. For example, coral exoskeleton, composed primarily of CaCO<sub>3</sub>, plays a crucial role as support and protector for corals to resist bathycurrent in the ocean (Fig. 1a).<sup>15</sup> Inspired by this skeletal structure, we have developed a novel kind of organic-inorganic composite membranes decorated with minerals to improve the mechanical stability and the surface wettability in an all-round way.<sup>16-18</sup> The polymer membranes are designed to have mineral coatings on the surfaces instead of

embedding inorganic particles in polymer matrix via blending<sup>19</sup> or in situ generation.<sup>20</sup> To achieve this goal, an intermediate layer was firstly constructed on the membrane surfaces,<sup>21,22</sup> and then mineral coatings were fabricated through biomineralization processes, such as carboxyl-induced calcification<sup>16,17</sup> and amino-induced silicification.<sup>18,23</sup> However, the mineral coatings are mainly composed of uniform nanoparticles rather than a rigid film. This structure is not able to endow the composite membranes with curling resistance and surface wettability simultaneously, as like the coral exoskeleton. In this work, we demonstrate zirconia-wrapped membranes with enhanced curling resistance and surface wettability via a mussel-inspired polydopamine/polyethyleneimine (PDA/PEI) intermediate layer (Fig. 1b). The membranes are uniformly wrapped by a rigid ZrO<sub>2</sub> coating, and thus are endowed with outstanding anti-curling performance during the drying process as well as anti-shrinkage under elevated temperature. Meanwhile, the organic-inorganic composite membranes are constructed with superhydrophilic and underwater superoleophobic surfaces, ensuring distinctive separation performance in oil-in-water emulsions.

The PDA/PEI intermediate layer is crucial for the formation of ZrO<sub>2</sub> coating through mineralization, whose properties greatly determine the morphology and distribution of minerals in the prepared membranes. Our previous work indicates that PEI accelerates the deposition process and a cross-linked PDA/PEI layer forms on the surfaces via Michael addition or Schiff-base reactions.<sup>22</sup> This layer is thinner, smoother, and more stable under alkaline environment than the pure PDA one. It can also chelate Zr<sup>4+</sup> from aqueous solution by catechol groups and induce the growth of ZrO<sub>2</sub> via reaction (1) to (3).<sup>24</sup>



Furthermore, the PDA/PEI-deposited membranes show highly improved permeability to aqueous solution, enabling the salt solutions to diffuse and mineralize throughout the whole membranes. Fig. 1c-e shows the surface morphologies for the membranes before and after mineralization. The membrane pores are slightly enlarged after deposited by the PDA/PEI layer. It is probably due to shrinkage induced by capillary pressure during the drying process. However, the ZrO<sub>2</sub>-wrapped membranes have similar aperture with the nascent one.

These morphologies indicate that the shrinkage can be overcome by the mineral coating in the composite membranes. Most importantly, it is easy to control the mineralization process just by tuning the hydrolysis conditions including pH, temperature and reaction time (Fig. S2 and Table S1, ESI<sup>†</sup>). Both high pH and temperature lead to thick mineral coatings and large particles because of the accelerated hydrolysis reaction. Compared to other minerals we reported before,<sup>16-18</sup> the ZrO<sub>2</sub> coating is more uniform and smooth without obvious evolution, which is similar to the polymer-in-a-silica-crust membranes reported by Wessling *et al.*<sup>25</sup>. The surface chemistry was analysed by XPS (Fig. 1f) and FT-IR (Fig. S3, ESI<sup>†</sup>) spectra, indicating the formation of PDA/PEI layer and ZrO<sub>2</sub> coating on the membrane surfaces. As shown in Fig. 1f, both N 1s and O 1s peaks arise after the co-deposition of PDA/PEI and the N/C ratio is approximate to one. The intensity of C 1s peak dramatically decreases, while the peaks assigned to O and Zr increase after mineralization. Moreover, the whole membranes can be uniformly mineralized as indicated by the elemental analysis of the cross-section (Fig. 1g and Fig. S4, ESI<sup>†</sup>), which is crucial for the structure stability and the surface wettability of the membranes discussed below. The density is higher than water for the mineralized membranes, while the nascent and PDA/PEI-deposited ones can float on the water surface, by which we can distinguish them easily (inserts in Fig. 1c-e).

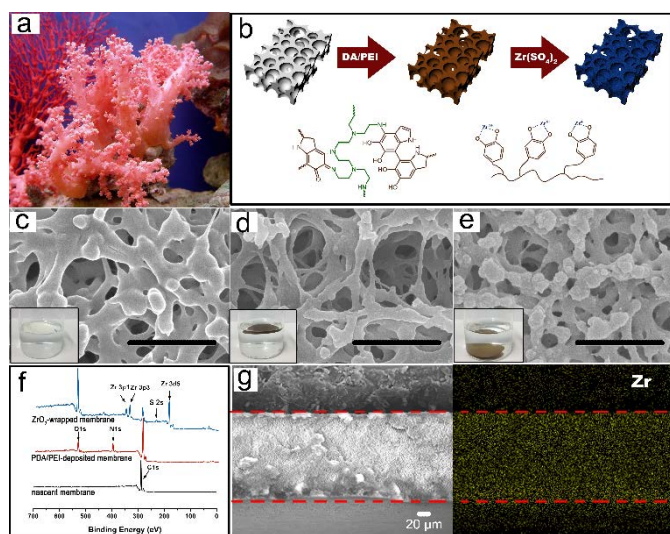


**Fig. 1** a) Digital photograph of corals in the ocean; b) Illustration of fabrication process for ZrO<sub>2</sub>-wrapped membranes; c) Surface morphologies of c) nascent, d) PDA/PEI-deposited and e) ZrO<sub>2</sub>-wrapped PP membranes; f) XPS spectra of the membrane surfaces; g) SEM and Zr element distribution images of the membrane cross-section. The scale bars in c-e are 1 μm.

Wetted membranes always suffer from unfavourable shrinkage or curling during the drying process. Macroscopic curling is also caused by non-isotropic shrinkage deriving from asymmetric structure or non-synchronous evaporation.<sup>26</sup> The driving force of shrinkage is capillary pressure ( $P_c$ ) in the pores (Fig. S5, ESI<sup>†</sup>), which can be calculated by the following equation:<sup>27</sup>

$$P_c = \frac{2\gamma \cos \theta}{r} \quad (4)$$

where  $\gamma$  is the interfacial tense of the air/water interface,  $\theta$  is the water contact angle of the surface, and  $r$  is radius of the pore. Obviously, the capillary pressure increases with the decline of

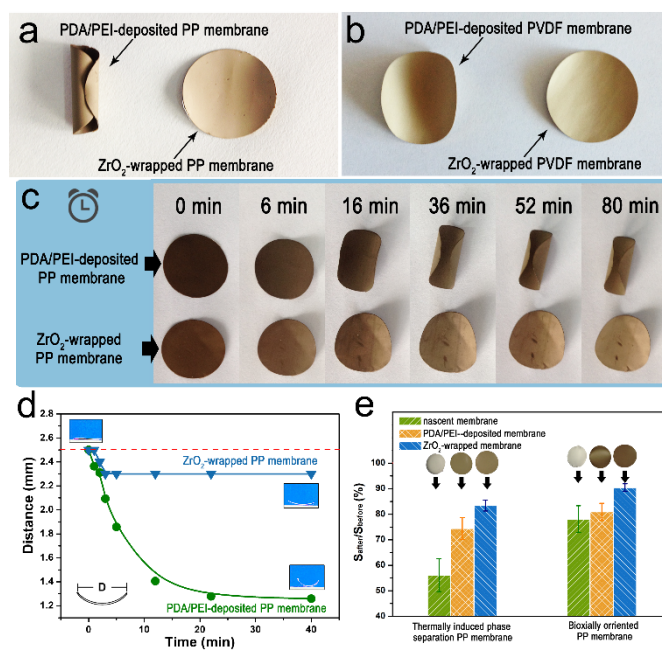


**Fig. 2** Digital photographs of a) PP and b) PVDF membranes dried in air; c) the drying process of PP membranes before and after mineralization; d) the distance between the edges against the time during the drying process of membranes; e) thermal shrinkage of PP membranes prepared by thermally induced phase separation and biaxial stretching.

water contact angle at the constant rate stage of evaporation. Therefore, the PDA/PEI-deposited membranes are hydrophilic and curl into rolls during drying in the air (Fig. 2a and b), because evaporation is faster at the top membrane surface than at the bottom one. It becomes more remarkable for those membranes with high porosity and soft skeleton. In contrast, the ZrO<sub>2</sub>-wrapped ones can resist deformation caused by the capillary pressure due to the rigidity and continuous structure of ZrO<sub>2</sub> mineral coating.<sup>28</sup> We monitored the drying process of polypropylene (PP) membranes as shown in Fig. 2c and d. The ZrO<sub>2</sub>-wrapped membranes have only a slight deformation while the PDA/PEI-deposited ones continue to curl during the drying process. This outstanding curling resistance is originated from high hardness and reduced modulus of the ZrO<sub>2</sub> coating in the composite membranes.<sup>23,29</sup> Composite structure can also promote the thermal stability of polymer membranes under elevated temperature. For example, Kang *et al.* reported silica-decorated separators with excellent resistance to thermal shrinkage.<sup>30</sup> Therefore, we compared the thermal stability of PP membranes fabricated via thermally induced phase separation and biaxial stretching (which has been widely used to fabricate Li-ion battery separators), respectively. The thermally induced phase separation membranes shrink more dramatically than the biaxial oriented ones when treated under 140 °C, because the former membranes have higher porosity than the later ones (Fig. 2e). More specifically, the ZrO<sub>2</sub>-wrapped membranes have area retention ( $S_{after}/S_{before}$ ) of 83% (for membranes by thermally induced phase separation) and 90.48% (for membranes by biaxial stretching), while the corresponding values are 56% and 78% for the nascent ones, respectively. The anti-shrink property of membranes has also been improved after deposited with PDA/PEI layer ( $S_{after}/S_{before}$  is 74% and 80%), attributed to its tough crosslinking network. Besides, the ZrO<sub>2</sub>-wrapped poly(vinylidene fluoride) (PVDF) membranes also show

enhanced resistance to the thermal-induced curling at high temperature (Fig. S6 and S7, ESI†).

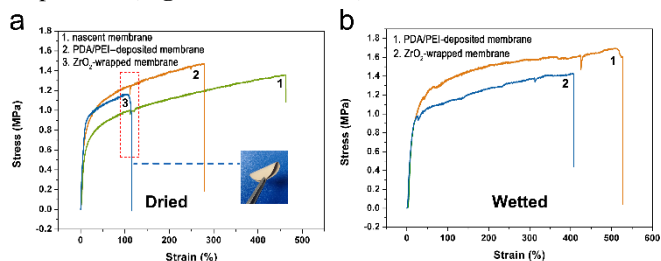


**Fig. 3** The stress-strain curves of PP membranes in a) dried and b) wetted states, respectively.

On the other hand, brittleness is another problem for rigid materials always faced during applications. We measured the mechanical property of the nascent and the mineralized membranes by the stress-strain test. Fig. 3 shows that the elongation at break declines to about 110% for the ZrO<sub>2</sub>-wrapped membranes, though they are more flexible than the inorganic membrane (insert in Fig. 3). A slight peak also appears around this point for the nascent and the PDA/PEI-deposited membranes, arising from the crack of some microstructures in the membranes. The results indicate that the mineral coating can not only improve the structural stability but also embrittle the membrane skeleton to a certain extent. Nevertheless, the membranes become much tough and “soft” after wetted by water. The elongation at break increases to 410% for the ZrO<sub>2</sub>-wrapped membranes in wetting state. Therefore, these membranes can satisfy the requirement of mechanical strength during pressure filtration for water treatment, and resist the unfavorable deformation during drying process.

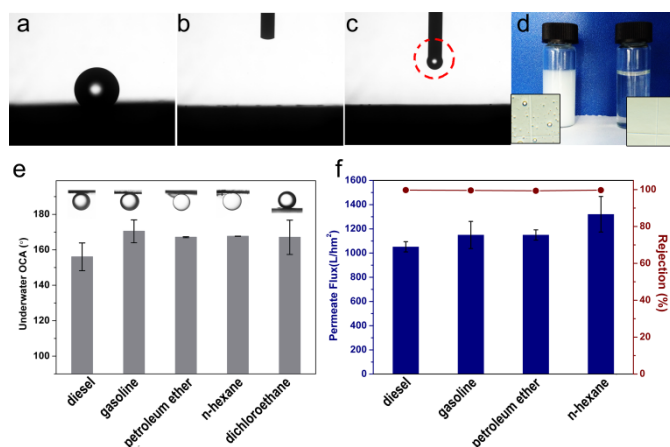


**Fig. 4** Water contact angles of a) nascent, b) PDA/PEI-deposited and c) ZrO<sub>2</sub>-wrapped PP membranes; d) the photograph of diesel-in-water emulsion and filtrate; e) Underwater oil contact angles of ZrO<sub>2</sub>-wrapped PP membranes; f) Permeate flux and rejection of oil-in-water emulsions separation.

The wettability is also greatly improved due to the natural hydrophilicity of ZrO<sub>2</sub> minerals. As shown in Fig. 3a, the nascent PP membranes is hydrophobic with a static water contact angle (WCA) above 120°. It declines to zero after the deposition of PDA/PEI layer.<sup>22</sup> The ZrO<sub>2</sub>-wrapped membranes also show an apparent WCA of zero, and the water drop permeates through the sample as soon as it contacts the membrane surface. A tiny droplet hangs on the needle top, which has been also observed when a drop contacts a water surface. It can be rationalized by the strong drawing force from the membrane surface (Fig. S8, ESI†), and the break of droplet

happens near the substrate with a residual drop on the needle.<sup>31,32</sup> All these results indicate that the ZrO<sub>2</sub>-wrapped membranes are superhydrophilic. These superhydrophilic membranes are great promising in oil/water separation.<sup>33-36</sup> They show outstanding oil resistance to various oils including diesel, gasoline, petroleum ether, n-hexane and dichloroethane. The underwater oil contact angles (OCA) are all above 160° (Fig. 3d). We also employed them for oil-in-water emulsion separation, and the membranes show both high rejection (above 99%) and permeate flux (above 1000 L·h<sup>-1</sup>·m<sup>-2</sup>) under relative low operation pressure (0.04 MPa) with excellent antifouling property, as shown in Fig. 3e (Fig. S9, ESI†).

In summary, we prepare ZrO<sub>2</sub>-wrapped membranes via a mineralization process on PDA/PEI coated substrates inspired by the composite structures of coral exoskeleton. Both the structure stability and the surface wettability of the membranes are greatly improved due to the rigid and hydrophilic mineral coating. Commercial filters and separators can benefit from the enhanced curling and thermal stability in practical applications. The as-prepared membranes have been also employed in oil-in-water emulsion separation with excellent performance. Moreover, the mineralized membranes can retain the original flexibility and structures of polymer membranes, which provides a promising solution to address the aforementioned contradictory in membrane hydrophilization.

## Notes and references

MOE Key Laboratory of Macromolecular Synthesis and Functionalization, Department of Polymer Science and Engineering, Zhejiang University, Hangzhou, 310027, China. E-mail: xuzk@zju.edu.cn

The authors thank financial support to this work by the Zhejiang Provincial Natural Science Foundation of China (Grant no. LZ15E030001) and the National Natural Science Foundation of China (Grant no. 50933006) and the National Undergraduate Scientific and Technological Innovation Project (Grant no. 20141033509412). We also acknowledge Prof. Lin Li from Beijing Normal University for the kind supply of polypropylene separators.

† Electronic Supplementary Information (ESI) available: [details of any supplementary information available should be included here]. See DOI: 10.1039/c000000x/

- M. A. Shannon, P. W. Bohn, M. Elimelech, J. G. Georgiadis, B. J. Marinas, A. M. Mayes, *Nature*, 2008, **452**, 301.
- P. Arora, Z. Zhang, *Chem. Rev.*, 2004, **104**, 4419.
- G. Metreveli, L. Wågberg, E. Emmoth, S. Belák, M. Strømme, A. Mihranyan, *Adv. Healthcare Mater.*, 2014, **3**, 1546.
- G. M. Geise, H.-S. Lee, D. J. Miller, B. D. Freeman, J. E. McGrath, D. R. Paul, *J. Polym. Sci. Pol. Phys.*, 2010, **48**, 1685.
- M. -H. Ryou, Y. M. Lee, J. -K. Park, J. W. Choi, *Adv. Mater.*, 2011, **23**, 3066.
- D. Rana, T. Matsuura, *Chem. Rev.*, 2010, **110**, 2448.
- J. F. Hester, P. Banerjee, A. M. Mayes, *Macromolecules*, 1999, **32**, 1643.
- A. Akthakul, R. F. Salinaro, A. M. Mayes, *Macromolecules*, 2004, **37**, 7663.
- M. Ulbrich, G. Belfort, *J. Appl. Polym. Sci.*, 1995, **56**, 325.
- K. S. Kim, K. H. Lee, K. Cho, C. E. Park, *J. Membr. Sci.*, 2002, **199**, 135.
- A. Bhattacharya, B.N. Misra, *Prog. Polym. Sci.*, 2004, **29**, 767;
- M. Ulbrich, G. Belfort, *J. Membr. Sci.*, 1996, **111**, 193.
- Č. Stropnik, V. Musil, M. Brumen, *Polymer*, 2000, **41**, 9227.

- 14 B. Sundaray, F. Bossard, P. Latil, L. Orgéas, J. Y. Sanchez, J. C. Lepretre, *Polymer*, 2013, **54**, 4588.
- 15 D. J. Barnes, *Science*, 1970, **170**, 1305.
- 16 P.-C. Chen, L.-S. Wan, Z.-K. Xu, *J. Mater. Chem.*, 2012, **22**, 22727.
- 17 P.-C. Chen, Z.-K. Xu, *Sci. Rep.*, 2013, **3**, 2776.
- 18 H.-C. Yang, J.-K. Pi, K.-J. Liao, H. Huang, Q.-Y. Wu, X.-J. Huang, Z.-K. Xu, *ACS Appl. Mater. Interfaces*, 2014, **6**, 12566.
- 19 G. G. Kumar, P. Kim, K. S. Nahm, R. N. Elizabeth, *J. Membr. Sci.*, 2007, **303**, 126.
- 20 X. Li, X. Fang, R. Pang, J. Li, X. Sun, J. Shen, W. Han, L. Wang, *J. Membr. Sci.*, 2014, **467**, 226.
- 21 B. C. Bunker, P. C. Rieke, B. J. Tarasevich, A. A. Campbell, G. E. Fryxell, G. L. Graff, L. Song, J. Liu, J. W. Virden, G. L. McVay, *Science*, 1994, **264**, 48.
- 22 H.-C. Yang, K.-J. Liao, H. Huang, Q.-Y. Wu, L.-S. Wan, Z.-K. Xu, *J. Mater. Chem. A*, 2014, **2**, 10225.
- 23 Z. Wang, X. Jiang, X. Cheng, C.H. Lau, L. Shao, *ACS Appl. Mater. Interfaces*, 2015, **7**, 9534.
- 24 Y. Mi, J. Wang, Z. Yang, Z. Wang, H. Wang, S. Yang, *RSC Adv.*, 2014, **4**, 6060.
- 25 A.M. Urmeny, A.P. Philipse, R.G.H. Lammertink, M. Wessling, *Langmuir*, 2006, **22**, 5459.
- 26 B. Li, Y.-P. Cao, X.-Q. Feng, H. Gao, *Soft Matter*, 2012, **8**, 5728.
- 27 C. J. Brinker, G. W. Scherer, *Sol-gel Science: The Physics and Chemistry of Sol-gel Processing*, Academic Press, 1990, pp. 454.
- 28 K. Guo, H. Song, X. Chen, X. Du, L. Zhong, *Phys. Chem. Chem. Phys.*, 2014, **16**, 11603.
- 29 D. H. Gracias, G. A. Somorjai, *Macromolecules*, 1998, **31**, 1269.
- 30 S. M. Kang, M.-H. Ryou, J. W. Choi, H. Lee, *Chem. Mater.*, 2012, **24**, 3481.
- 31 O. A. Basaran, *AIChE J.*, 2002, **48**, 1842.
- 32 B. Ambravaneswaran, O. A. Basaran, *Phys. Fluids*, 1999, **11**, 997.
- 33 Z. Xue, S. Wang, L. Lin, L. Chen, M. Liu, L. Feng, L. Jiang, *Adv. Mater.*, 2011, **23**, 4270.
- 34 W. Zhang, Y. Zhu, X. Liu, D. Wang, J. Li, L. Jiang, J. Jin, *Angew. Chem. Int. Ed.*, 2014, **53**, 856;
- 35 S. J. Gao, Z. Shi, W. B. Zhang, F. Zhang, J. Jin, *ACS Nano*, 2014, **8**, 6344.
- 36 F. Zhang, W. B. Zhang, Z. Shi, D. Wang, J. Jin, L. Jiang, *Adv. Mater.*, 2013, **25**, 4192.